

Highly recyclable EDTA-crosslinked chitosan-gelatin biopolymer adsorbent for the separation and recovery of rare earth elements from aqueous solution

Monu Verma¹, Deepa Sachan¹, Vinod Kumar^{2,5}, Waseem Ahmad⁴, Nishesh Sharma³, Hyunook Kim^{1*}

¹Department of Environmental Engineering, University of Seoul, Seoul, 02504, Republic of Korea

²Department of food science & Technology, Graphic Era (Deemed to Be University), Dehradun, Uttarakhand 248002, India

³Department of Chemistry, Uttaranchal University, Dehradun, Uttarakhand, 248007, India

⁴Department of Chemistry, Graphic Era (Deemed to Be University), Dehradun, Uttarakhand 248002, India

⁵Peoples' Friendship University of Russia (RUDN University), Moscow 117198, Russian Federation

*Corresponding author:

Hyunook Kim: h_kim@uos.ac.kr

Text SI – 1: *Materials and reagents*

All reagents were of analytical grade and were used as received without further purification. Chitosan flakes (+ 85% deacetylated), with molecular weight of 190000–375000 g/mol and a viscosity of 200–2000 MPa, gelatin, and ethylenediaminetetraacetic acid (EDTA, 99%) were purchased from Sigma-Aldrich (Seoul, Republic of Korea). Pyridine (99.5% purity) and acetic anhydride (98% purity) were obtained from Daejung, Republic of Korea. Lanthanum nitrate hexahydrate ($\text{La}(\text{NO}_3)_3 \cdot 6\text{H}_2\text{O}$, 99.99%), Cerium nitrate hexahydrate ($\text{Ce}(\text{NO}_3)_3 \cdot 6\text{H}_2\text{O}$, $\geq 99\%$), and Europium nitrate hydrate ($\text{Eu}(\text{NO}_3)_3 \cdot 6\text{H}_2\text{O}$, 99.99%) were purchased from Sigma-Aldrich (Seoul, Republic of Korea). All the experiments were performed using deionized (DI) water.

Text SI – 2: *Material characterization*

The structure and surface morphology were investigated through field-emission scanning electron microscopy (FESEM) (SU-8010, Hitachi, Japan) at a working voltage of 10.0 kV voltage. The elemental composition was examined using a Thermo Scientific Ultra Dry SDD equipped with an FESEM. The crystalline phase, structure, and purity of the synthesized chitosan, gelatin and prepared CS-EDTA-GL were analyzed through high resolution powder X-ray diffraction (PXRD)

employing Bruker AXS D8 advance, Germany, using monochromatic Cu K α radiation ($k = 1.54 \text{ \AA}$). The scan rate was kept $2^\circ/\text{min}$, with a step size of 0.02° in the range of $5^\circ\text{--}80^\circ$ with an operating voltage of 40 kV and 30 mA at room temperature. Fourier transform infrared spectroscopy (FT-IR) (Nexus 670, Thermo Electron Corporation, USA) was used in the range of $400\text{--}4000 \text{ cm}^{-1}$ to examine the surface functional groups on the adsorbent surface. BelsorpX mini (MicrotracBEL Corp., Japan) instrument was used to investigate the specific surface area, pore size, and pore volume of the used adsorbent at 77.35K in 0.0–1.0 range of relative pressures during the N₂ adsorption–desorption isotherm performance. The surface areas and pore size distributions were calculated using the Brunauer–Emmett–Teller (BET) and Barrett–Jones Halenda (BJH) methods, respectively. The EXSTAR 6300, (Japan) instrument was used to conduct the thermogravimetric analysis (TGA) and derivative thermogravimetric (DTG) with a heating rate of $10^\circ\text{C}/\text{min}$ from 40°C to 700°C in N₂ environment. X-ray photoelectron microscopy (XPS) was conducted on PHI Versa Probe III, USA, using Al K α radiation source (1486.708 keV, step width = 0.05 eV, pass energy = 55 eV, base pressure of 10^{-7} mbar). The REE concentrations before and after the experiments were quantitatively determined through inductively coupled plasma optical atomic emission spectrometry (ICP – OES, Model ICAP 7000) instrument (Thermo Fisher Scientific, USA).

Text SI – 3: *Details of batch adsorption experiments*

3.1. Batch adsorption experiments

Stock solutions of REEs La (III), Ce (III), and Eu (III) were prepared, and all experiments were performed by taking 20 mg of adsorbent with 20 mL of pollutant solutions in 50 mL centrifuge tubes to investigate the adsorption behavior (including solution pH, adsorption kinetics and isotherms, and selectivity). The effect of solution pH on the REE recovery was investigated with concentrations of 100 mg/L in the pH range 2.0–7.0. During the pH experiment, pH 6.5 and 7.7 were also selected due to their similarity to the pH range of seawater (6.50–8.05, Ellis et al., 2014). Above 8.0 pH, alkaline solutions (pH > 8) were not examined to prevent the formation of metal hydroxide precipitates. Adsorption kinetics experiments were performed at an initial concentration of 100 mg/L and contact time intervals of 0, 5, 10, 20, 30, 60, 90, 150, 240, and 360 min. In isotherm experiments, initial concentrations range of REEs were selected as 1–100 mg/g with equilibrium time 360 min to obtain equilibrium. During the kinetic and isotherm experiments, the pH was fixed at 6.0. The solution pH was adjusted using buffer solutions and 0.1 mol/L NaOH or 0.1 mol/L HNO₃. Then, the suspension tubes were shaken continuously in shaker (Maxshake™, Daihan Scientific, Republic of Korea) at 230 r/min at 25°C to obtain adsorption equilibrium. The adsorbent was separated from the solution using 0.45 μm polypropylene syringe filter and diluted using 2% HNO₃, and the residual concentrations of REEs were quantitatively determined through inductively coupled plasma optical atomic emission spectrometry (ICP–OES, Model ICAP 7000) instrument (Thermo Fisher Scientific, USA). All the experiments were conducted three times under the same conditions, and average mean \pm standard deviations (SD) were used for

calculations. The amounts of REEs adsorbed onto specific adsorbents at time t and at equilibrium were calculated using the following equations (Eq. (S1) and (S2)):

$$\text{Adsorption capacity } (q_e) = \frac{(C_0 - C_e) \times V}{m}, \quad (\text{S1})$$

$$\text{Adsorption capacity } (q_t) = \frac{(C_0 - C_t) \times V}{m}, \quad (\text{S2})$$

where C_0 (mg/L), C_t (mg/L), and C_e (mg/L) are the initial, time t , and equilibrium concentration of the target pollutant in solution, respectively. q_t (mg/g) and q_e (mg/g) represent the adsorption capacity of a specific adsorbate at time t and at equilibrium, respectively. V (mL) is the volume of the sample solution, and m (g) is the amount of adsorbent used for adsorption.

3.2. Adsorption in multi-component REE systems

To investigate the competitive adsorption of the used REEs, La(III), Ce(III), and Eu(III), onto the CS-EDTA-GL adsorbent, a multi-component system experiment was conducted using similar initial concentrations of each type of REEs ranging from 1 to 100 mg/L. To obtain the maximum adsorption capacity of REEs by the adsorbent, an initial pH value of 5.0 was used based on the results from the monocomponent system. A contact time 4.0 h was selected to achieve proper adsorption equilibrium for the multi-component experiment.

3.3. Adsorption selectivity test

For the selectivity test, a mixture of 16 different REEs Ce (III), Dy (III), Er (III), Eu (III), Gd (III), Ho (III), La (III), Lu (III), Pr (III), Sc (III), Sm (III), Tb (III), Tm (III), Y (III), and Yb (III) with initial concentration of each 2.0 mg/L was prepared. Subsequently, 10 mg adsorbent was dispersed in 10 mL under the optimized experimental conditions obtained by monocomponent system. After 4.0 h of shaking, the adsorbent was filtered out, and the concentrations of REEs in the solution were determined through ICP-OES. Finally, the separation effect of CS-EDTA-GL on the REEs was evaluated by calculating the separation factors (β) under different concentration conditions between the REEs.

3.4. Reusability test

In the regeneration experiments, 50 mg adsorbent was treated with 20 mL of 50 mg/L initial solution concentration of each La(III), Ce(III), and Eu(III) solution. After 4.0 h, when the adsorption equilibrium was reached, the adsorbing material was filtered and washed using 10 mL of 1.0 mol/L HNO₃ to regenerate, neutralized using DI water, and dried in a vacuum oven for the next cycle. This process was repeated for five continuous cycles in the regeneration experiment.

3.5. Adsorption Performance of CS-EDTA-GL in pure water, tap water and industrial wastewater

Four different types of water (pure water, tap water, and two industrial wastewater samples) were selected for this experiment. The first industrial wastewater (I₁) was collected from Miryang, Changwon (influent), and the second industrial wastewater (I₂) was collected from Miryang, Gumi (influent), Republic of Korea. The different physicochemical properties, such as pH, TOC, TS, VS, and TP, of the I₁ and I₂ wastewaters were determined using the Standard Methods (APHA) according to OECD guidelines in our established research and development (R&D) center, Jungnang, Republic of Korea, and are listed in Table S1. Both industrial wastewaters were filtered using 0.45 µm membrane and used as a solvent for experiments. All samples were spiked with La (III), Ce (III), and Eu (III) to final concentrations of 100.0 µg/L, and then 50 mg adsorbent was mixed 50 mL REEs samples and shaken in a rotary oscillator at ~150–155 r/min at 25°C for 4.0 h. Subsequently, the adsorbing material was separated using 0.45 µm membrane and acidified with 2% HNO₃ for ICP analysis.

Text SI-4: Adsorption isotherm models

4.1. Adsorption kinetics models: Two well-known adsorption kinetic models, the pseudo-first-order (PFO) and pseudo-second-order (PSO) kinetic models, were fitted to the kinetic data to further calculate the relevant kinetic parameters

(i) **Pseudo – first – order kinetics model:** The PFO kinetics model is described in a nonlinear form (Eq. (S3)):

$$q_t = q_e(1 - e^{-k_1 t}) \quad , \quad (S3)$$

where q_e (mg/g) and q_t (mg/g) are the amounts of REEs adsorbed at equilibrium and time t (min), respectively. k_1 (per min) is the first-order sorption kinetic constant.

(ii) **Pseudo – second – order (PSO) kinetics model:** The PSO kinetics model is described in a nonlinear form (Eq. (S4)):

$$q_t = \frac{k_2 q_e^2 t}{1 + q_e k_2 t} \quad , \quad (S4)$$

where q_e (mg/g) and q_t (mg/g) are the adsorption capacities of the adsorbent for REEs at equilibrium and at time t (min), respectively, and k_2 (g/mg·min) is the second-order adsorption rate constant.

(iii) **Webber–Morris intraparticle diffusion model:** The Weber–Morris model describes film or pore diffusion as the controlling step of the adsorption process, which is described as (Eq. (S5))

$$q_t = k_i t^{0.5} + C \quad , \quad (S5)$$

where q_t (mg/g) is the amount of adsorbed REEs at time t (min), k_i (mg/g·min^{0.5}) is the diffusion rate constant, and C is the intercept, which provides an indication of the boundary layer thickness.

4.2. Adsorption Isotherms models: Two famous isotherm models:

Langmuir and Freundlich were applied on isotherm data

Langmuir isotherm model: This model is widely applicable to homogeneous adsorption surfaces, where each of the adsorption sites can only bind one adsorbate (Touihri et al., 2021). The nonlinear form of the Langmuir model is given in Eq. (S6):

$$q_e = \frac{q_m K_L C_e}{1 + K_L C_e} \quad , \quad (S6)$$

where q_e and q_m indicate the equilibrium and maximum adsorption capacities of the used adsorbate (mg/g), respectively. C_e in mg/L and K_L in L/mg are the equilibrium concentrations of REEs used in the aqueous phase and the Langmuir constant concerning the adsorption energy, respectively.

Freundlich isotherm model: This model assumes a heterogeneous surface and non-uniform distribution of adsorption heat over the surface without saturation of adsorption sites (Jaiswal et al., 2021). The nonlinear form of the Freundlich model is represented by Eq. (S7).

$$q_e = K_F C_e^{1/n} \quad , \quad (S7)$$

where q_e in mg/g and C_e in mg/L represent the adsorption capacity of the adsorbate and the equilibrium REE concentration in the aqueous phase, respectively; and K_F ((mg/g)·(L/mg)^{1/n}) and n are the Freundlich constants, which represent the adsorption amount and adsorption intensity, respectively. The magnitude of the n values reflects whether the uptake characteristics are good ($2 < n < 10$), difficult ($1 < n < 2$), or poor ($n < 1$).

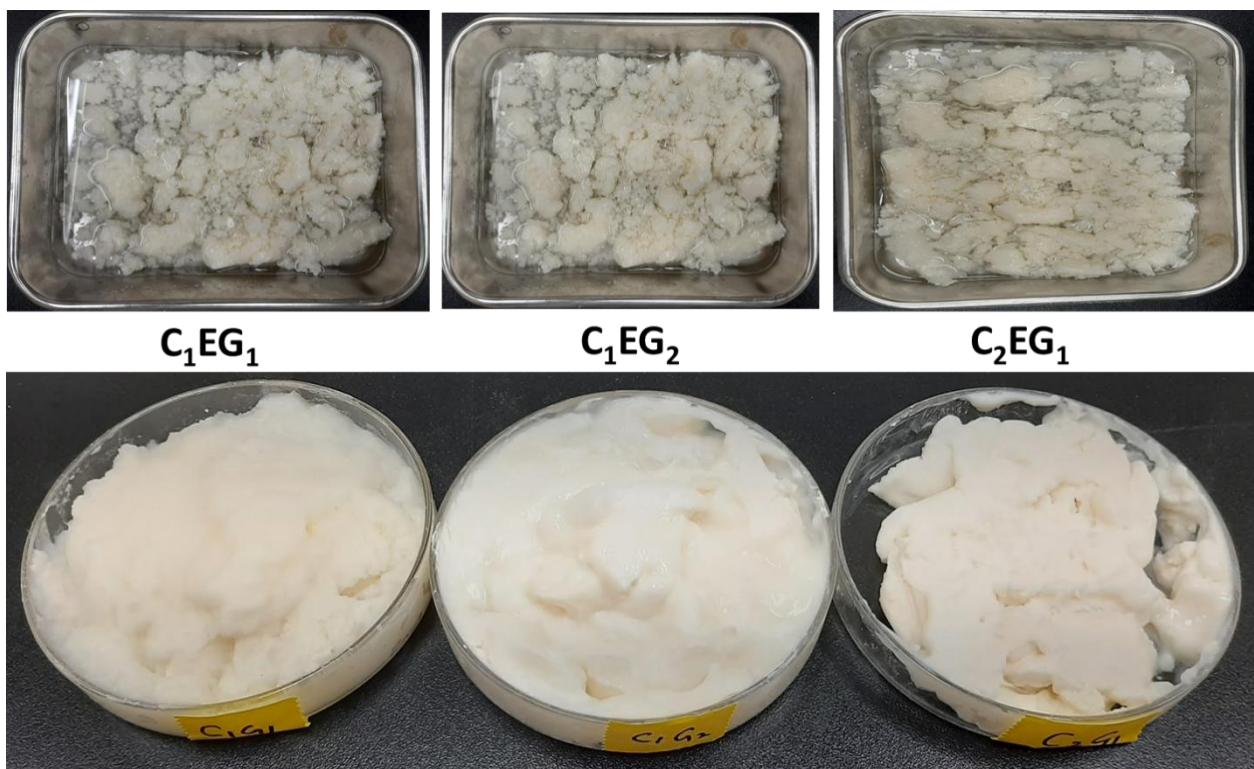


Fig. S1 Three CS-EDTA-GL adsorbent synthesized with three different ratios of 2:1, 1:2, and 1:1.

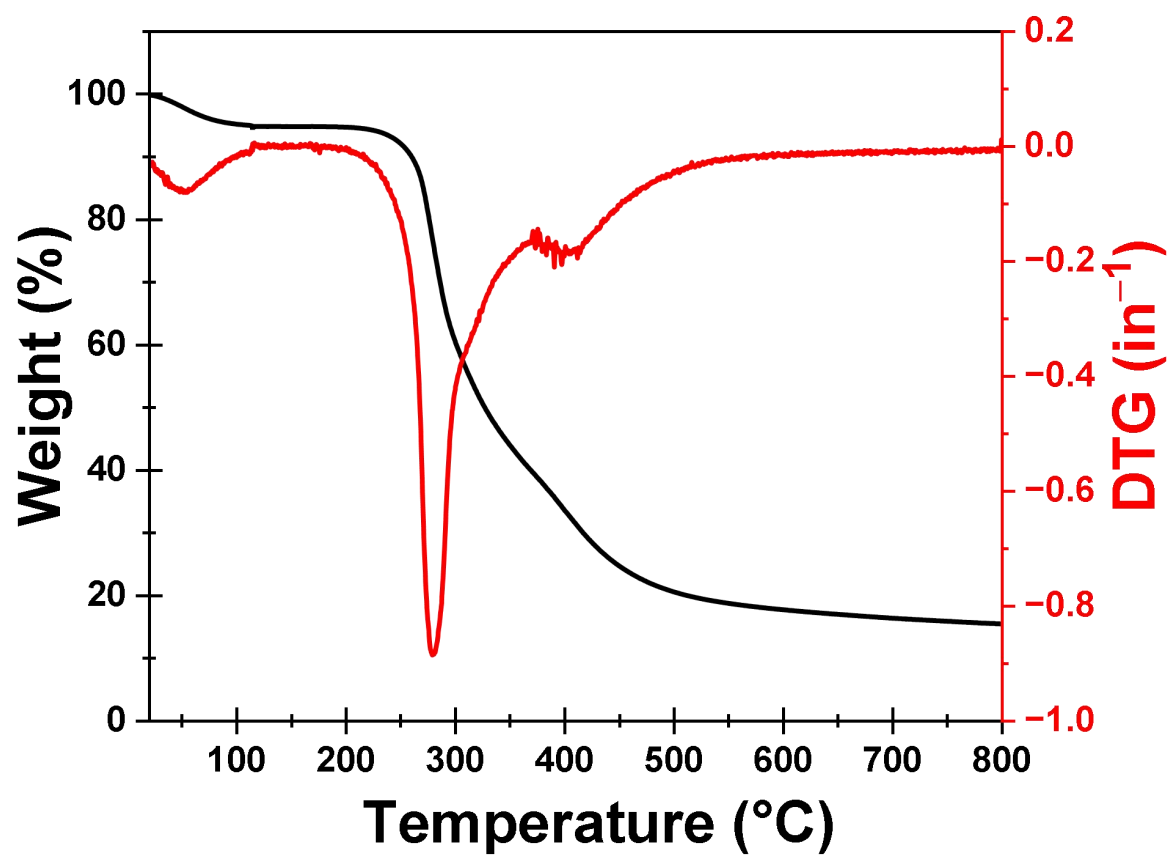


Fig. S2 TGA and DTG curves of CS-EDTA-GL adsorbent.

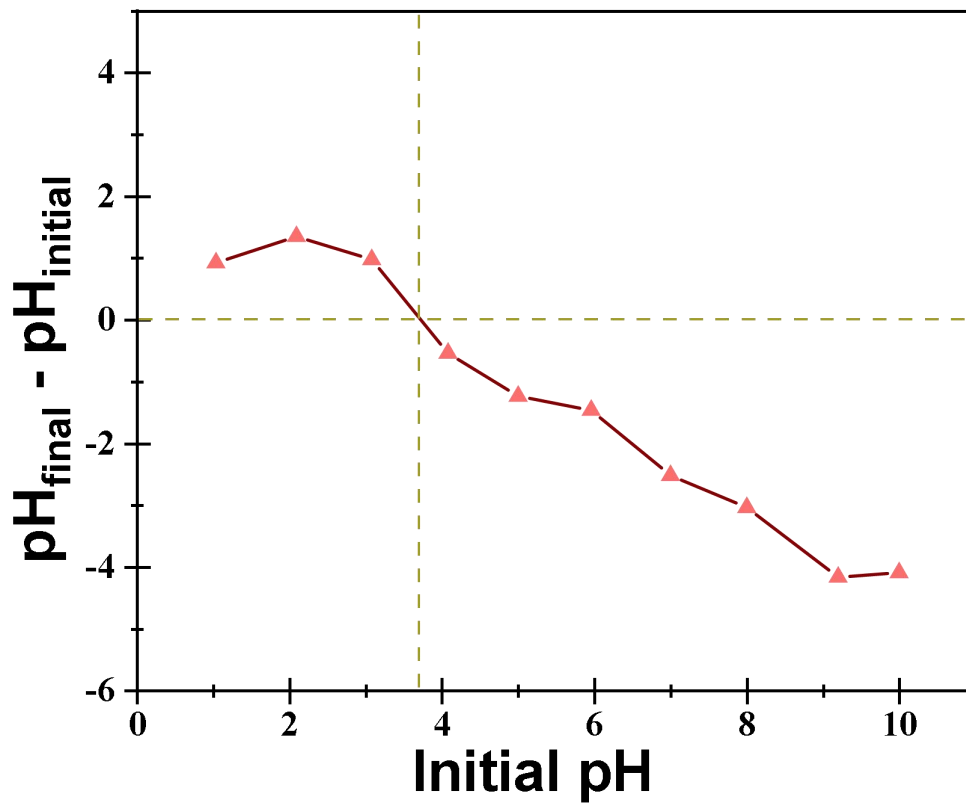


Fig. S3 Point of zero charge (Pzpc) of the CS-EDTA-GL adsorbent examined using pH drift method.

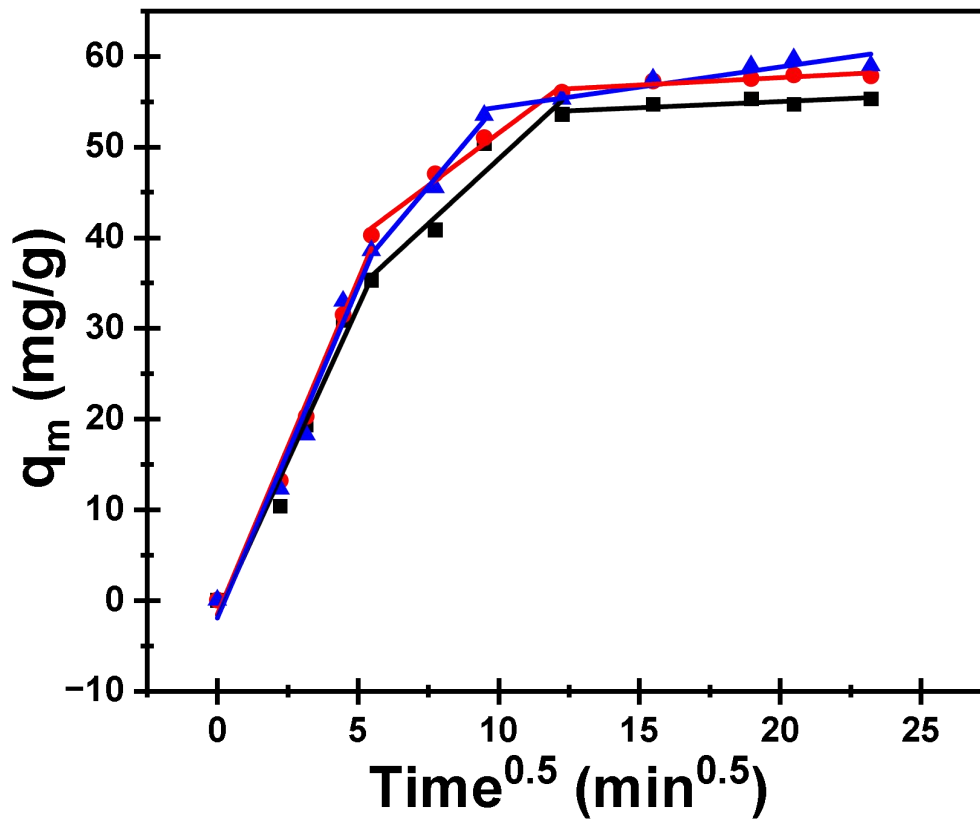


Fig. S4 Webber–Morris kinetics intraparticle diffusion model in the REE adsorption onto CS-EDTA-GL adsorbent.

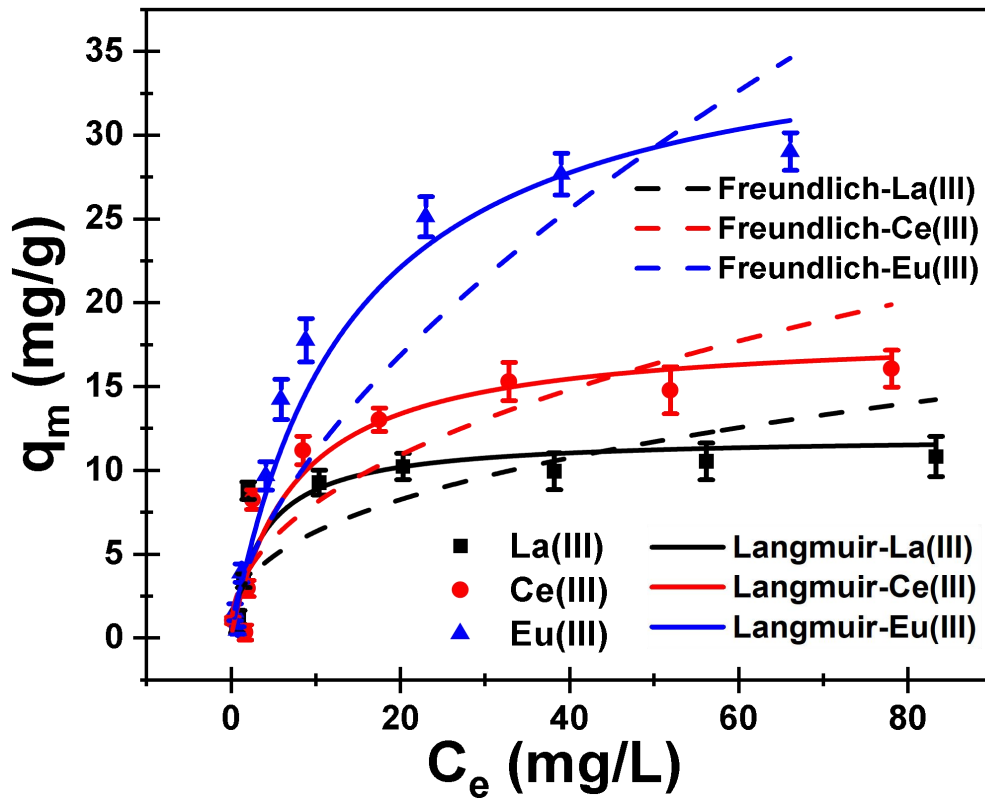


Fig. S5 Modeling of multi-component adsorption of REEs onto CS-EDTA-GL adsorbent.

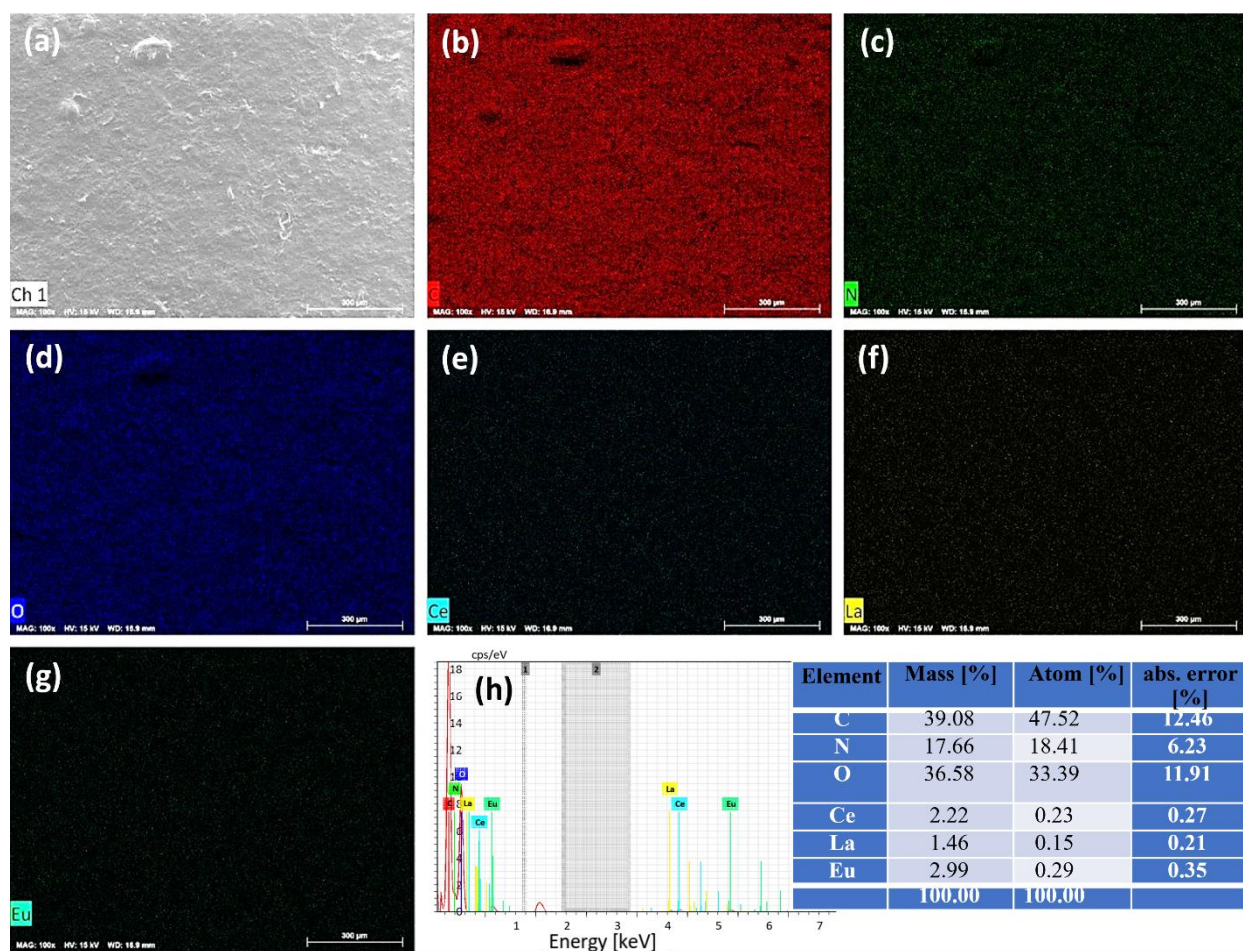


Fig. S6 EDS mapping image of CS-EDTA-GL after mixed La(III), Ce(III), and Eu(III) adsorption; FESEM image highlighting the region used for EDS analysis (a), C K mapping (b), N K mapping (c), O K mapping (d), Ce L mapping (e), La L mapping (f), Eu L mapping (g), and EDS spectra and elemental composition (h).

Table S1 Initial and final concentrations of REEs in different types of waters.

Type of water	Initial Concentration ($\mu\text{g/L}$)		
	La(III)	Ce(III)	Eu(III)
Pure Water	98	96	102
Tap Water	94	97	102
WW1	92	97	98
WW2	95	94	90
Type of water	Final Concentration ($\mu\text{g/L}$)		
	La(III)	Ce(III)	Eu(III)
Pure Water	1	1.3	0.5
Tap Water	1.25	2.40	0.75
WW1	3.2	4.60	2.7
WW2	4.6	6.7	4.35

References

- Ellis R P, Spicer J I, Byrne J J, Sommer U, Viant M R, White D A, Widdicombe S (2014). ¹H NMR metabolomics reveals contrasting response by male and female mussels exposed to reduced seawater pH, increased temperature, and a pathogen. *Environmental Science & Technology*, 48(12): 7044–7052
- Jaiswal K K, Kumar V, Vlaskin M S, Nanda M, Verma M, Ahmad W, Kim H (2021). Hydropyrolysis of freshwater macroalgal bloom for bio-oil and biochar production: Kinetics and isotherm for removal of multiple heavy metals. *Environmental Technology & Innovation*, 22: 101440
- Touihri M, Guesmi F, Hannachi C, Hamrouni B, Sellaoui L, Badawi M, Poch J, Fiol N (2021). Single and simultaneous adsorption of Cr(VI) and Cu (II) on a novel Fe₃O₄/pine cones gel beads nanocomposite: Experiments, characterization and isotherms modeling. *Chemical Engineering Journal*, 416: 129101